Materials and Structures
DOI 10.1617/s11527-015-0623-5

ORIGINAL ARTICLE

Daily and seasonal thermal stresses in tilings: a field survey combined with numeric modeling

R. Zurbriggen · M. Herwegh

Received: 7 November 2014 / Accepted: 27 April 2015

Abstract This study investigates thermally induced tensile stresses in ceramic tilings. Daily and seasonal thermal cycles, as well as, rare but extreme events, such as a hail-storm striking a heated terrace tiling, were studied in the field and by numerical modeling investigations. The field surveys delivered temperature–time diagrams and temperature profiles across tiling systems. These data were taken as input parameters for modeling the stress distribution in the tiling system in order to detect potential sites for material failure. Dependent on the thermal scenario (e.g., slow heating of the entire structure during morning and afternoon, or a rapid cooling of the tiles by a rain storm) the modeling indicates specific locations with high tensile stresses. Typically regions along the rim of the tiling field showed stresses, which can become critical with respect to the adhesion strength. Over the years, ongoing cycles of thermal expansion–contraction result in material fatigue promoting the propagation of cracks. However, the installation of flexible waterproofing membranes (applied between substrate and tile adhesive) represents an efficient technical innovation to reduce such crack propagation as confirmed by both numerical modeling results and microstructural studies on real systems.

Keywords Ceramic tilings · Temperature induced expansion · Thermal shrinkage · Finite element modeling · Failure

1 Introduction

Temperature variations along daily or seasonable cycles induce expansions and contractions in building materials. Depending on the type of material and extend of such temperature variations, over the years the material can fatigue and may result in damage by the onset of brittle failure. For that reason various studies investigated the link between thermal variations and material failure for different building materials (e.g. [3, 4, 8, 10, 13, 14]). In the case of externally applied building materials, in many climate zones they are exposed to daily or seasonal temperature changes in the order of 30 °C. Especially facade or flooring composite-systems with layers of different materials undergo thermal stresses at their adhesive interfaces. Passa et al. [11] studied an external thermal insulation system composed of expanded polystyrene boards protected by a cementitious render. Both materials undergo very different thermal strains, which lead to cracking. According to Felixberger [2] thermally induced length changes of ceramic tiles can generate shear stresses higher than

R. Zurbriggen (✉)
R&D Department, Akzo Nobel Chemicals AG,
Industriestrasse 17a, 6203 Sempach Station, Switzerland
e-mail: roger.zurbriggen@akzonobel.com

M. Herwegh
Institute of Geological Sciences, University of Bern,
3012 Bern, Switzerland

Published online: 08 May 2015

0.5 MPa, which on a long-term can become critical and cause failure. Beside thermal loads, a ceramic tiling can be stressed by drying induced shrinkage of the tile adhesive and/or the substrate. Especially in cases of young screeds or concrete substrates shear stresses can become critical, as well [2].

The influence of such hygrical loadings (by repeated wetting and drying) on the microstructure and properties of outdoor tilings was investigated by Wetzel et al. [16, 17]. Herwegh et al. [5] carried out a finite element analysis on the stress distribution in the adhesive mortar and grout as a function of application system and substrate shrinkage. Two of the major findings were that, firstly, hollows in the mortar bed cause local stress concentrations, which in case of the floating technique might initiate micro-cracks at the interface and provoke failure. Secondly, the flexible waterproofing membrane can strongly reduce stresses in the adhesive mortar and the grouts in case of substrate shrinkage. Both of these findings confirm existing technical recommendations related to material selection, system design and tile installation procedures. To mention is the industrial standard DIN18157-1, where for outdoor tiling applications the combined buttering-floating technique is recommended. Thereby the adhesive mortar is trowelled onto the substrate (floating), as well as onto the rear side of the tile (buttering). This ensures an optimum wetting of the tile's rear side and a durable adhesion between mortar and tile. Another recommendation is the application of a flexible waterproofing membrane (German: Verbundabdichtung, see [19], Merkblatt ZDB) in between substrate (screed or concrete) and tile adhesive. This membrane blocks water migration across the tiling system and has the capability to over-bridge cracks formed in the substrate. Due to its low elastic modulus it acts as a deformable layer between the rigid substrate and tiles.

The present paper focuses on the effects of frequent thermal loadings caused by daily and seasonal temperature cycles and on rare but extreme events such as a hail-storm. The former have the potential to cause fatigue failure by the accumulation of hundreds to thousands of cycles over the years, while the latter may cause cracking by the high intensity of single events. Once (micro-) cracks are formed, the material properties such as the thermal coefficient and elastic modulus can increase and decrease, respectively, which might accelerate deterioration [12].

In this context Yiu et al. [18] tested experimentally the relationship between thermal–moisture weathering cycles and shear strength of external wall tile systems. Samples and laboratory weathering conditions are very close to real wall tilings and natural weathering conditions as they occur in the Hong-Kong area (tropical transitional climate). They tested shear strength of the tile-adhesive interface and found it to be reduced by 50 % after 100 weathering cycles, which were interpreted to simulate 50 years of durability (two cycles per year). Furthermore, strain estimates of Yiu et al. [18] indicate that the surface of the tile is thermally expanding much stronger than the interface between tile and adhesive.

Mahaboonpachai et al. [6] did a laboratory study on the degree of tile delamination as a function of the temperature of the tile surface. Their conclusion is rather general suggesting that cyclic thermal loadings caused by sun radiation can lead to delaminations. Mahaboonpachai et al. [7] investigated the interfacial fracture toughness as a critical parameter to predict the crack propagation mechanism leading to delamination.

In contrary to the laboratory studies of Mahaboonpachai and coworkers, we performed a field experiment with real outdoor tilings over the period of 3 years including real-time monitoring of thermal and failure evolution. This field experiment delivered all data for this study. In a first part, data of several field surveys are reported to demonstrate typical temperature–time curves and gradients across a tiling system. In the second part, typical heating and cooling events, as they were observed in the field, were taken as a base for stress calculations by the finite element program ABAQUS. Thereby, material properties and geometric aspects of the real tilings of the field experiment were taken as input parameters for the numerical modeling. The resulting spatial distributions of elastic stress of the different events are then discussed in the context of their frequency as they occur throughout the year. Finally, the authors try to come up with suggestions how to counteract the generation of critical stresses in outdoor applied ceramic tilings.

2 Methods

2.1 Temperature and thermal expansion measurements in field experiment

For the field experiment the different walls, floor and roof (with a thickness of 9 cm) of a prefabricated

concrete garage served as substrates for the tilings. The set-up is shown in Fig. 1 and described in Zurbriggen et al. [21] and in Wetzel et al. [17]. The outdoor tilings on the south-west wall and the balcony floor tiling on the roof of the garage are most relevant for this study, because the south-west wall represent a typical weathering facade and the open balcony (without roof) allows to study effects of thunder storms such as standing rain and hail ice.

During application works, thermo-couples were installed at predefined places in the concrete substrate, in the mortar layer, inside the tile and on the tile's surface (Fig. 1b). This was done for selected tiles on the south-west wall and the balcony. The same tiles were equipped with plug gauges for dilatation measurements with a so-called "deformater" [15]. These plug gauges were fixed with epoxy glue in a distance of 20 cm (i) within the tiles, (ii) between neighboring tiles across the grout (see Fig. 1d of [17]) and (iii) on corresponding opposite locations on the concrete walls inside the garage. The latter allowed the measurement of the surface temperature and related thermal expansion of the concrete back-wall.

2.2 Finite element method for calculation of the spatial distribution of stresses

With the finite element code ABAQUS Version 6.9 (see references in [5]) thermally induced elastic stresses in a balcony tiling were calculated. The experiments consisted of four mechanical parts: porcelain tiles, adhesive mortar (and grout), waterproofing flexible membrane and a concrete substrate. The geometric and thermo-mechanical input parameters of these parts (Fig. 2; Table 1) were taken in analogy to the field experiment: a tiling field with a width of 273.2 cm, composed of nine fully vitrified ceramic tiles porcelain tiles (type B-Ia, EN 14411) measuring 30 cm × 30 cm and 8 mm in thickness, with 4 mm cementitious grouts (class CG2, EN 13888) in between, applied on a 4 mm thick mortar bed (class C2, EN12004), applied on a 2 mm thick flexible waterproofing membrane (class A01, A02, B0, [20], Merkblatt ZDB), applied on a 90 mm thick concrete substrate (450 kg/m^3 CEM I 42.5 R; w/c ∼ 0.47; 47.5 N/mm^2 compressive strength). To reduce calculation time, we restricted to 2D space and

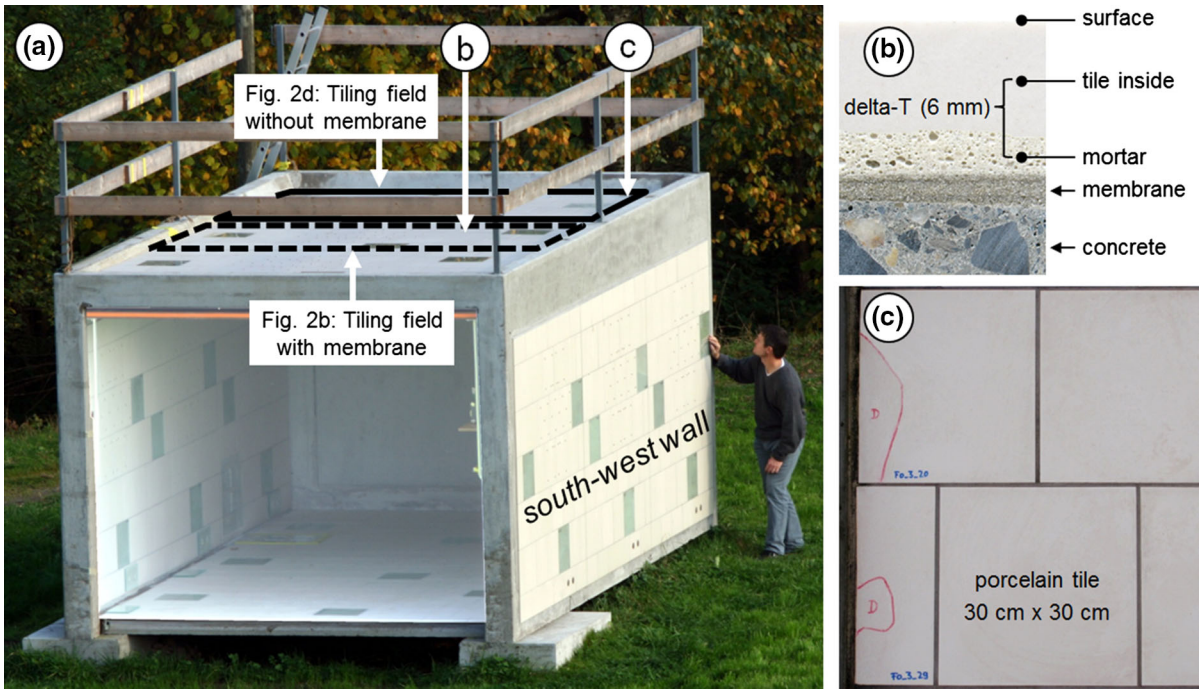

Fig. 1 **a** Prefabricated garage provides walls and floors on the *inside* and *outside* as substrate for tilings. **b** Cross-section through floor tiling on the roof (balcony) with indicated positions of thermo-couples at the surface of the tile, in the middle of the tile and in the middle of the mortar bed. **c** Localised detachments along the rim of the tiling field

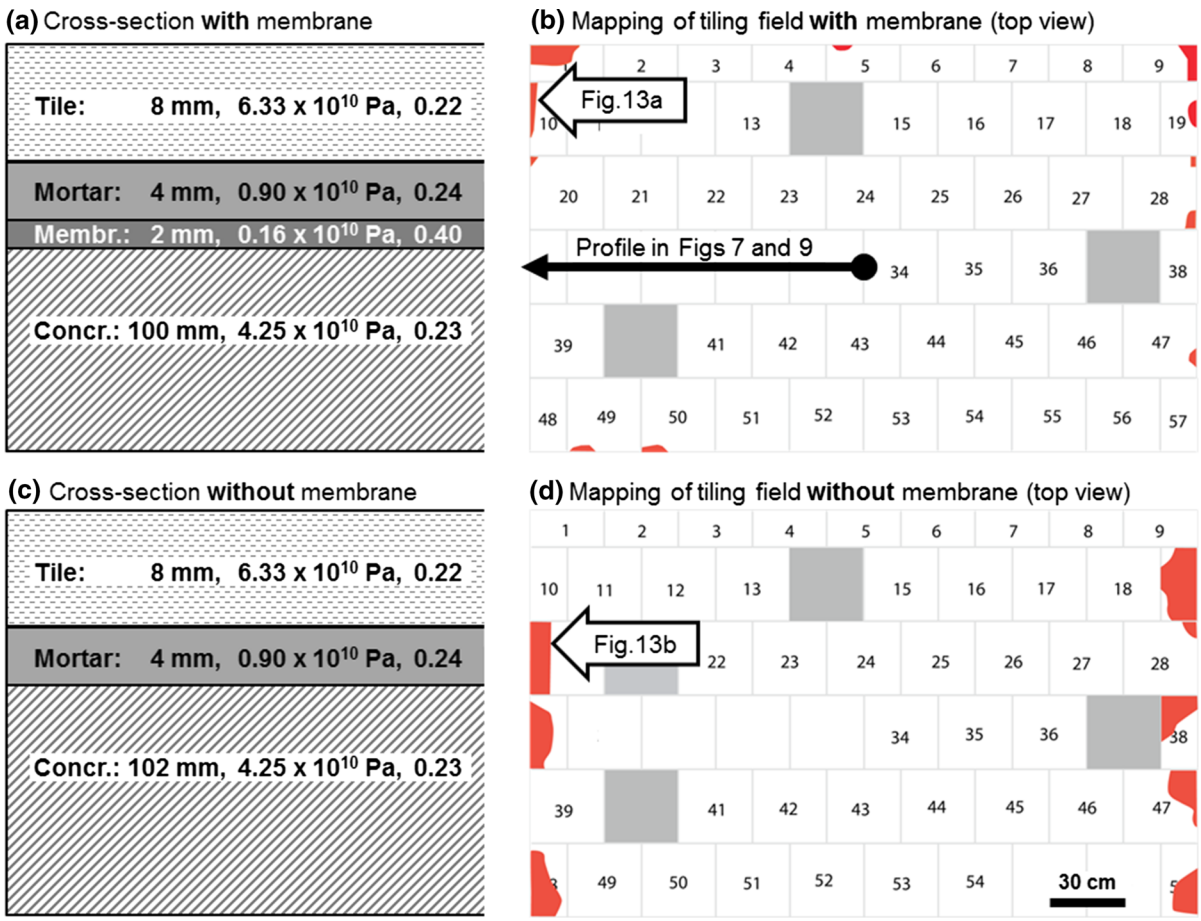

Fig. 2 System setups (**a**, **c**) with geometric and thermo-mechanical parameters for each material, such as layer thickness, *E* modulus, Poisson ratio, and mappings of corresponding tiling sectors (**b**, **d**) of the field experiment as located in Fig. 1

only one half of the balcony tiling system was modeled. The detailed setup is illustrated in Fig. 2 of Herwegh et al. [5].

For finite element modeling square meshes were used (for dimensions see [5]). We only used elasticity and neither creep nor brittle or ductile fracturing was incorporated. Also no evolution of material fatigue was implemented. These simplifications are justified since we only intend to detect the location of stress concentrations due to thermal expansion/contraction. The validity of the modeling results was evaluated by comparing the locations of high stress with the positions of crack initiation as observed in the case of the outdoor experiment. A reduction to a pure elastic analysis is further justified by shear force–deformation curves of tile adhesives which are quasi linear. In fact, linearity can be observed until *c*. 80 % of strength, where the elastic limit is reached. Beyond that, the curves are slightly bent before the material fails. Thus, plasticity of tile adhesives can typically be observed in the last 20 % of loading before break.

Since we restrict the modeling to pure elastic response on temperature changes, Young's moduli, Poisson ratios and thermal coefficients for each part were used (see Fig. 2; Table 1). Consequently, any temperature change resulted in an instantaneous adaptation of the stress state in the model and no time versus temperature evolutions were integrated. However, we indirectly treat fast and slow cooling/heating scenarios. For slow long-term cooling/heating, the entire system was subjected to temperature change without spatial thermal gradients. In this way, expansion/contraction between the different parts depend directly on differences in the thermal coefficients. In contrast, for fast

Table 1 Setups and measured material properties used for the different numerical models

	Thickness (mm)		Thermal expansion coefficient (10^{-6} K^{-1})		Material properties	
	Setup without membrane	Setup with membrane	Slow heating or cooling	Fast heating or cooling	*E* modulus (GPa)	Poisson ratio
Tile	8	8	5.8	5.8	63.3	0.22
Grout	4	4	10	0	9	0.24
Mortar	4	4	10	0	9	0.24
Membrane	0	2	200	0	1.6	0.40
Concrete	102	100	6.4	0	42.5	0.23

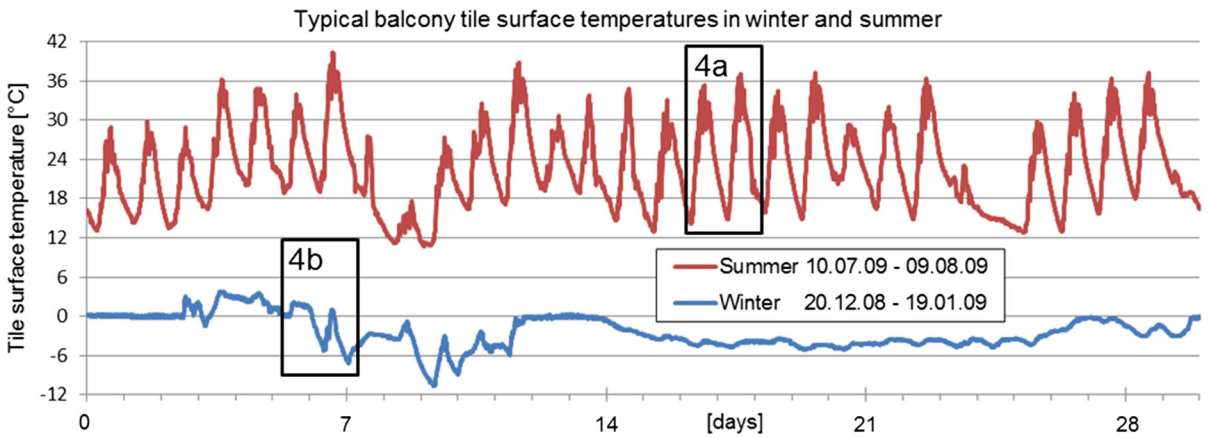

Fig. 3 Temperature variations at the surface of a bright balcony tile over a period of 30 days in summer (*upper curve*) and winter (*lower curve*)

cooling/heating, only the tiles were allowed to cool/heat. Hence thermal contraction/expansion of the tile forced the model parts below the tile to react in a pure elastic manner.

Beside the geometry of the tiling elements, the material properties of Table 1 were further input parameters for the modeling.

2.3 Transmitted light microscopy of failure locations

Failure sites were selected on the base of periodical observations and quantitative mappings as described in Wetzel et al. [17]. First, these failure sites were impregnated on site with stained epoxy resin. This procedure allowed in a second step to cut out samples without the risk that the samples fall apart along the existing cracks. Thirdly, thin-sections were prepared as described in Wetzel et al. [16].

3 Results

3.1 Temperature measurements in the field

The surface temperature of a tile depends on a number of factors related to (i) illumination (angle of inclination, duration of illumination, intensity which can be decreased by shadows of clouds, trees or building elements), (ii) the environment (temperature, humidity, strength and direction of wind), (iii) in case of weathering, temperature and intensity of rain, hail or snow (iv) the physical properties of the tile (luminance as a measure for the reflectance, mean bulk temperature, conductivity, heat capacity, thickness) and (v) the physical properties of the substrate materials (mean bulk temperature, conductivity, heat capacity, thickness).

To overcome this complexity, we carried out a field survey and measured surface temperatures of tiles

Table 2 For selected tile materials (natural stones, ceramics and glass), the corresponding thermal expansion coefficients (left column), the maximum heating amplitude observed on the SE wall during 22nd March 2011 (middle column) and the calculated thermal expansions are listed (right column)

Material	Thermal expansion coefficient (10^{-6}/K)	Heating amplitude on 22nd March 2011 (°K)	Calculated thermal expansion (mm/m)
Limestone	3.8	33.4	0.13
Granite	4.2	35.4	0.15
Semi-vitrified	4.8	33.8	0.16
Bright porcelain	5.8	36.8	0.21
Dark porcelain	5.8	42.8	0.25
Float glass	7.1	36.4	0.26

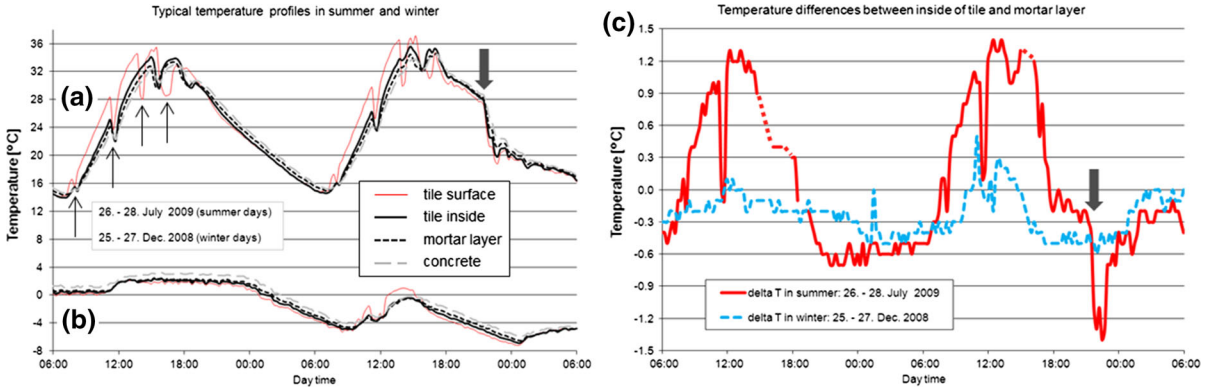

Fig. 4 Typical temperature profiles of 2 selected days in summer (**a**) and winter (**b**). The corresponding differences in temperatures between the inside of the tile and the mortar layer are shown in diagram (**c**). Note that the discrete coolings (indicated by *thin arrows* in **a**) are related to shadows of a railing on *top* of the garage (see Fig. 1a). They appear always at the same daytime. *Thick arrows* in **a** and **c** indicate the same rainstorm

throughout the year. The location of the field experiment is north of the Alps in central Switzerland (coordinates: 47.1163985° northern latitude/8.2048533° eastern longitude/511 m altitude) and is representative for a mid-European transitional climate with a minimum daily mean temperature of 0 °C in winter, a maximum daily mean temperature of *c*. 18 °C in summer and rain/snow quantities between 65 mm/month in winter up to 150 mm/month in summer [9]. Figure 3 shows two selected sequences of 30 days, one typical for winter and another typical for summer seasons. It is to mention that the measured tiles were relatively bright (Fig. 1). Note that surfaces of dark tiles would additionally heat up by at least 5 °C (see Table 2) reaching maximum temperatures of *c*. 45–50 °C during a hot summer day. Generally, the amplitude of balcony tile surface temperatures in summer (±15 °C) is twice as high than in winter (±8 °C). If floor tiles are covered by snow, then the daily amplitude can become even smaller than one degree (see Fig. 3).

Figure 4 shows typical daily temperature profiles of a balcony tiled with bright beige ceramic tiles. It becomes evident that the largest temperature gradient is between the surface of the tile and its inside (measured in the mid of a 8 mm thick tile). Typically, a daily temperature profile is asymmetric: morning heating is stronger, thus, the temperature of the tiling rises faster compared to the continuous but slow cooling during night (Fig. 4a). Therefore, the temperature difference between the inside of the tile and the mortar reaches a daily maximum of 1.4 °C just after noon, while the nightly cooling causes a low temperature difference of −0.7 °C only (Fig. 4c). Most interesting is the temperature-effect of the rainstorm at 21:30 h of the 27th July 2009 (indicated by a thick arrow in Fig. 4a). This abrupt cooling caused a

temperature difference between the inside of the tile and the mortar of −1.4 °C (indicated by a thick arrow in Fig. 4c). During winter the absolute temperature variability (Fig. 4b) as well as the difference between the inside of the tile and the mortar is much less, in the order of 0.5 °C (stippled curve in Fig. 4c).

The survey of the 22nd of March 2011 provided a wealth of thermal data shown in Fig. 5. Following observations were made:

1. 22nd March, day and night are exactly 12 h. In this transitional season night temperatures can still fall below 0 °C, but day temperatures of tilings can reach temperatures of 25 °C (Fig. 5a, b, c, d).
2. Given by the northern latitude of 47.1° and the date (22nd of March), the sun inclinates at noon, theoretically, with an angle of 42.9° (complementary angle of geographic latitude). In fact, the measurement in the field provided this value for the balcony tiling (Fig. 5a). But for the wall exposed to south west, sunrise was at 10:30 h, 2½ hours later, and the sun inclination angle reached its maximum of 65° in late afternoon at 15:40 (Fig. 5b).
3. Even though the wall is 2.5 h shorter exposed to the sun its surface temperature reaches 25 °C (Fig. 5b), which is 7 °C more than in case of the balcony (Fig. 5a). The cause is the larger sun inclination angle, and thus, the higher intensity of sun radiation in case of the wall.
4. At 16:30 h a big shadow of a neighboring tall building hit both, balcony and SW wall and let the temperatures fall by 7 °C (indicated by black arrow in Fig. 5a, b). However, this relatively fast cooling did not generate a considerable temperature difference (named delta-*T* in Fig. 5a, b) between inside of tile and mortar layer. The highest delta-*T* of 1.2 °C occurs on the balcony just before noon (Fig. 5a).
5. Despite of the higher surface temperature, the delta-*T* (temperature difference between the inside

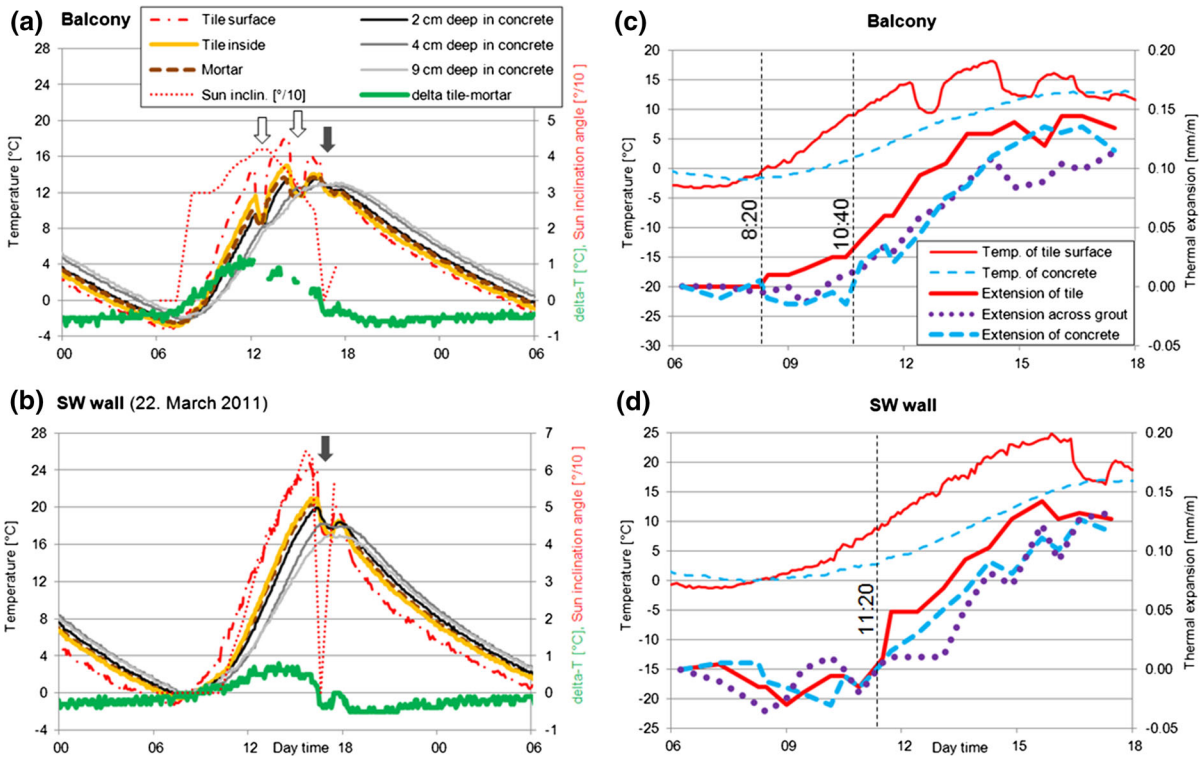

Fig. 5 Daily temperature profiles measured over 30 h (from midnight until 6 o'clock in the morning of the next day) of a balcony tiling (**a**) and a wall tiling (**b**; exposed to southwest) during 22nd of March 2011. *White arrows* mark *small shadows* of a building element and *black arrow marks large shadow* of a neighboring building. Diagrams **c** and **d** represent the corresponding thermal expansion data. Expansion was measured within the tile (*solid line*), across the grout (*dotted line*) and on the backside of the concrete floor and wall (*dashed line*). Note: temperature curves in **a** and **b** labeled "9 cm deep in concrete", and the temperature curves labeled "Temp. of concrete" in figures **c** and **d** are the same data

of the tile and the mortar) of the wall is significantly lower than that of the balcony (Fig. 5a, b).

6. Given by the larger angle of inclination of the sunlight, the wall is heated more and faster, but the thermal expansion of the wall tiles and the balcony tiles reach the same maximum value of 0.14 mm/m (Fig. 5c, d).
7. However, the difference in thermal expansion between tile and concrete substrate is larger for the balcony tiling (Fig. 5c, d). This observation is also confirmed by the larger delta-*T* (temperature difference between the inside of the tile and the mortar) in case of the balcony tiling (Fig. 5a, b).

The same thermal data of the 22nd March 2011 was analysed with respect to temperature profiles. The by far largest thermal gradients of up to 1 °C/mm occur in the outer half of the tile, whereas at the tile-mortar interface the gradients drop down to 0.2 °C/mm or even less.

These surveys indicate that, with respect to the thermal loads at the adhesion interface between tile and mortar, one can focus on the local temperature difference (delta-*T*) at this interface. In order to provide an impression on the annual distribution of the thermal loads, all available delta-*T* values of the balcony tiling between December 2008 and November 2009 were plotted in Fig. 6. It becomes evident, that the thermal loads are significantly stronger in summer than in winter. Note that the delta-*T* values strongly increase in April and May, which also explains why the crack propagation rate is highest during this period of the year as shown in Fig. 13 of Wetzel et al. [17]. Figure 6 furthermore demonstrates that the maximum delta-*T* value is 1.5 °C, even in case of an extremely fast cooling during a rain-storm. We therefore chose a maximum delta-*T* of 2 °C for following numeric modeling works.

3.2 Numerical modeling of spatial stress distribution in outdoor floor tilings undergoing thermal loading

Based on the field survey, we decided to differentiate between two thermal scenarios: (i) a slow and (ii) a fast scenario. (i) "Slow" means that heating or cooling occurs slowly with respect to the conductivity of the materials. Thus, a thermal gradient across the tiling system was ignored and the modeling calculates thermal stresses, which are created by the different thermal expansion coefficients of the involved materials, only. Slow heating and cooling was modeled over a temperature change of 30 °C. (ii) On the other hand, the "fast" scenario mimics a fast heating or cooling, which affects only the tiles but not the mortar and concrete substrate below the tiles. Therefore, the thermal coefficients of the mortar (adhesive and grout mortar), the flexible waterproofing membrane and the concrete were set to zero, and consequently any heating or cooling in the model is affecting only the tile. In analogy to real maximum temperature differences between mortar and the inside of tile of 1.5 °C, the numerical modeling of the elastic thermal stresses was carried out for fast heating or fast cooling of the tiles by 2 °C.

In the sake of simplicity, we regarded only elastic stresses as they can be calculated from the elastic moduli and Poisson rations of the materials (Table 1) as a function of the temperature change. Neither plastic nor brittle cracking were regarded during the numerical modeling. Thus, the modeling results will only indicate the locations where reversible elastic stresses occur.

Tensile stresses and shear stresses below 0.5 MPa are still well within the elastic regime of typical stress–strain curves of adhesive and grout mortars. Repeated loading and unloading within the reversible elastic regime (below 0.5 MPa) is not causing a permanent deformation and is therefore regarded to be uncritical on a long-term. On the other hand, stress cycles which regularly reach values above 0.5 MPa have the potential to cause fatigue failure. Especially, if they frequently occur over large numbers of daily cycles.

Figure 7a shows the stress distribution after a slow heating of 30 °C. Because the tiles have the smallest thermal coefficient, they suffer increasing tension from center to rim of the tiling field. The outermost 1.5 tiles undergo tensions of >1 MPa, but they are not critical with respect to the much higher tensile strength of a porcelain tile. The concrete and the mortar layers (adhesive and waterproofing membrane) are loaded in compression or low tension. Critical tension of 1 MPa is only generated in the peripheral grouts and in the mortar layer at the rim of the outermost tile.

In contrast, slow cooling of the balcony by 30 °C delivers a completely different stress distribution (Fig. 7b). The tiles are under low tension, but the mortar layers and the concrete are stressed much

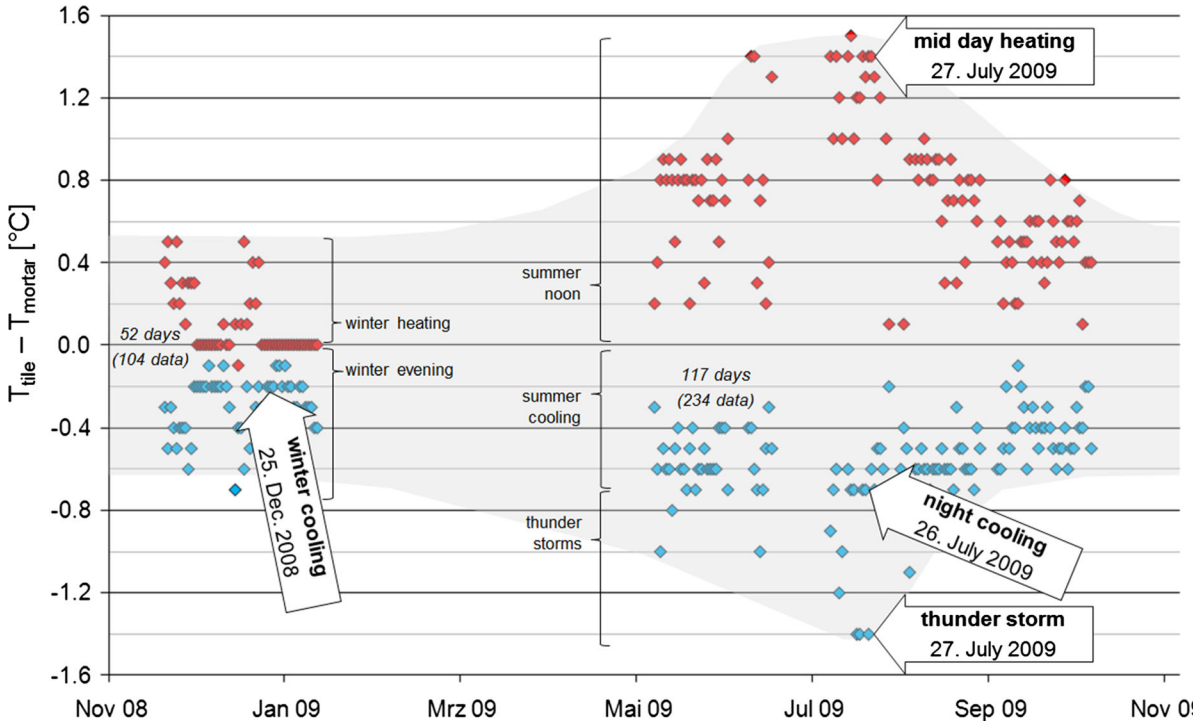

Fig. 6 Per day the maximum positive (heating during day) and maximum negative (cooling during night) difference in the temperature between the inside of the floor tile and the adhesive mortar are plotted over the period of 1 year. Data are missing from 20th Jan–14th May 2009 and from 12th Oct 2009 onwards. Typical events are indicated by *arrows*. Data taken from Wetzel et al. [17]

stronger. In addition, the stress gradient increases from the rim of the tiling field inwards. Especially in the adhesive mortar and in the waterproofing membrane stresses exceed 1 MPa.

Comparing the stresses in the grouts during heating and cooling it becomes evident, that the stress peak is at the surface and at the base of the grout when heated and cooled, respectively.

Figure 8a shows the stress evolution in the peripheral grout during heating and cooling by 30 °C. The shapes of the heating curves are steepening, while the cooling stress-curves are more of a flattening type. Therefore, heating stresses overcome cooling stresses when the change of temperature is high. But, when only heated or cooled by 10 °C, then the stresses are similarily low (<0.2 MPa).

The stress evolution in the adhesive mortar (Fig. 8b) is quite different. Here, the cooling generates much higher stresses, which can become critical (>0.5 MPa) when cooling is more than 15 °C.

Fast heating (only the tiles warm up; Fig. 9a) and fast cooling (only the tiles cool down; Fig. 9b) by 2 °C generate tensional stresses in the mortar, which generally are low. Only in the case of a fast cooling, tensions of 0.5 MPa might generate at the surface of the grouts.

4 Discussion

Figure 2 shows that maximum and minimum temperatures in summer and winter time, respectively, are about 40 °C and −10 °C. Therefore, the ideal application temperature would be at about 15 °C. The temperature surveys on the field experiment reveal that seasonal temperature changes are in the order of ±25 °C. The modeled slow heating (Fig. 7a) and slow cooling (Fig. 7b) scenarios therefore give insights into the evolution and spatial distribution of thermal stresses, information that cannot be gained from the field experiment alone. The slow cooling by 30 °C (Fig. 7b) indicates tensile stresses in the adhesive mortar of >1 MPa. If real "winter stresses" would be that high, then many balcony tilings would detach in

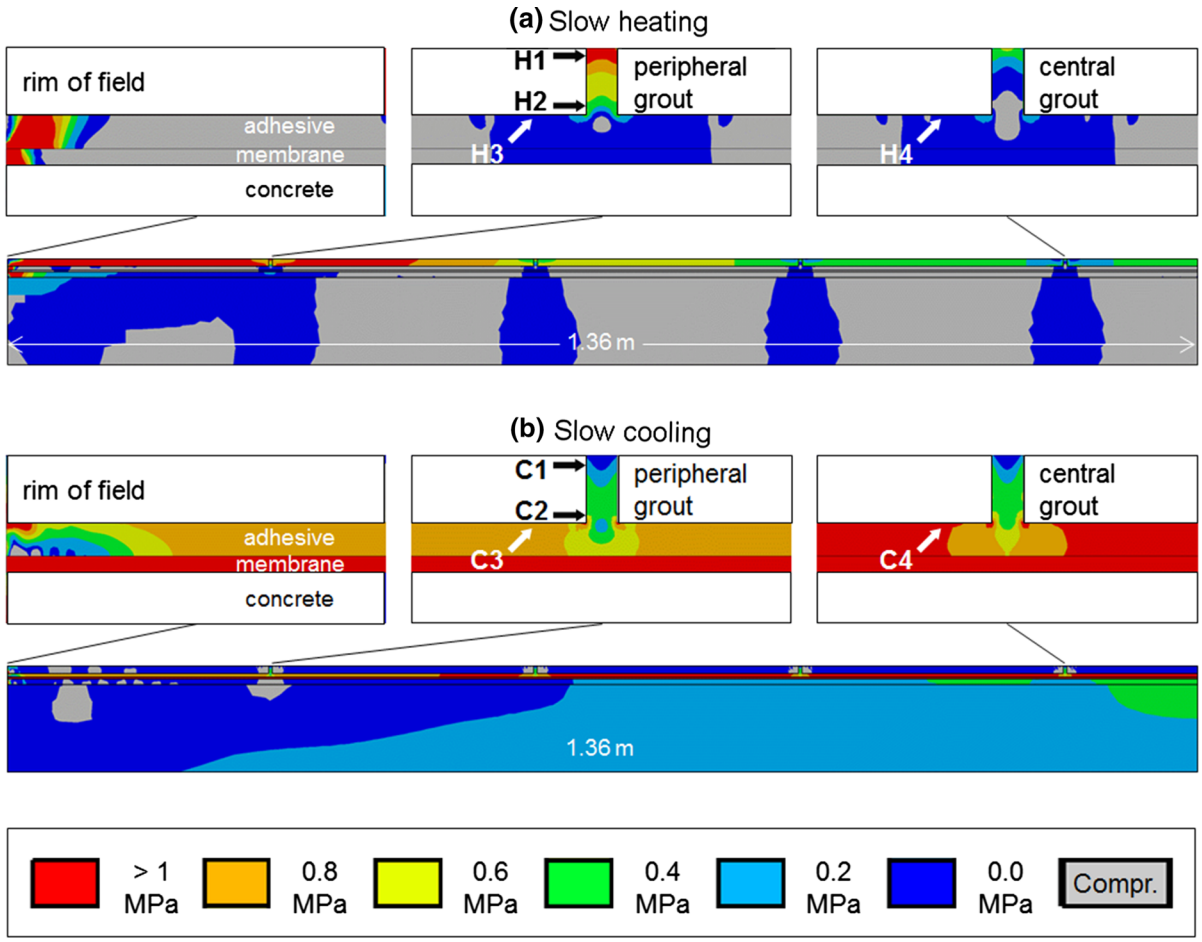

Fig. 7 Distribution of tensile stresses across one half of a tiling field (*left* rim of tiling field, *right* center of tiling field, as located in Fig. 2b). Stress distribution at the rim (*left inset*), in a peripheral grout (*middle inset*) and in a central grout (*right inset*) during (**a**) slow heating by 30 °C and (**b**) a slow cooling by 30 °C. The stress evolution during heating/cooling at the indicated locations H1-4 and C1-4 are shown in Fig. 8

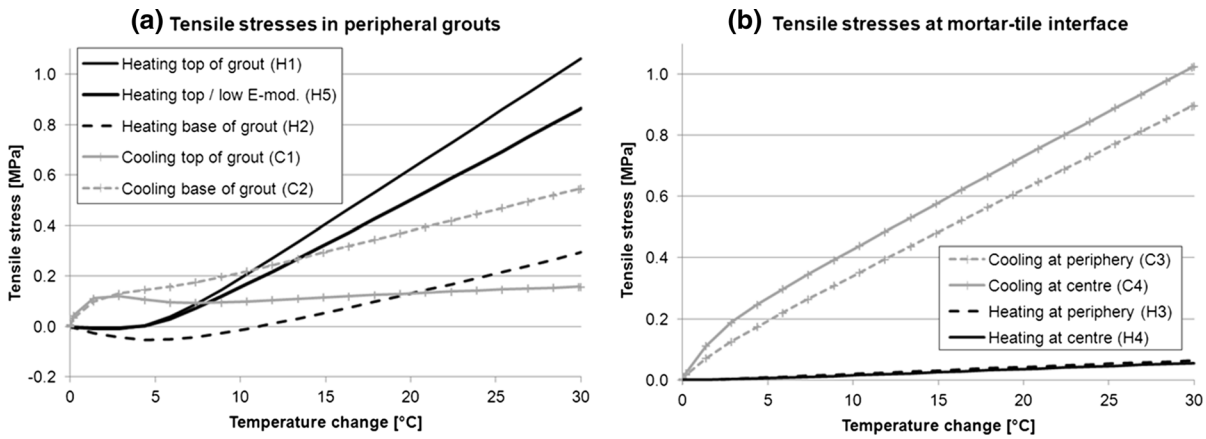

Fig. 8 Temperature-stress curves in peripheral grouts (**a**) and at the mortar–tile interfaces (**b**). Locations H1–H4 and C1–C4 are indicated in Fig. 7; location H5 is indicated in Fig. 10

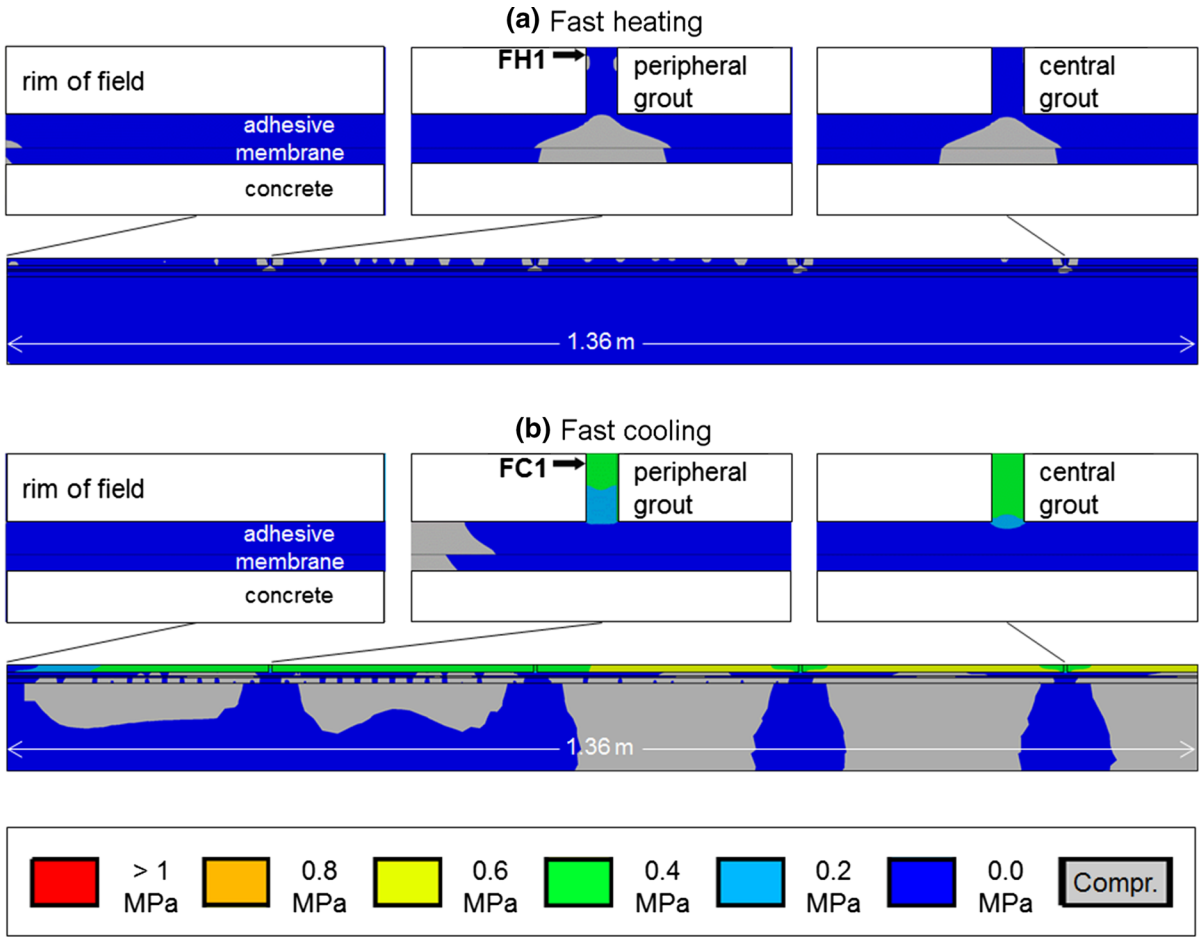

Fig. 9 Distribution of tensile stresses across one half of a tiling field (*left* rim of tiling field, *right* center of tiling field, as located in Fig. 2b). Stress distribution at the rim (*left inset*), in a peripheral grout (*middle inset*) and in a central grout (*right inset*) during (**a**) fast heating and (**b**) fast cooling. The modeled scenarios correspond to an abrupt exposure to sunlight (fast heating) and an abrupt cooling by a thunder storm, respectively

the first hard winter. Because this is not the case, plastic deformation and stress release by micro-cracking, which are not considered in the numerical modeling, may play a role. Therefore, the numerical models on the variations of elastic stress should be taken as an indication under which thermal conditions what kind of reversible maximum elastic stress concentrations may occur.

However, the numerical models clearly show that both, slow heating (Fig. 7a) and fast cooling (Fig. 9b) cause stress concentrations at the surface of peripheral grouts. In reality, a typical summer rain-storm in late afternoon will hit a heated terrace or balcony tiling corresponding exactly to the modeled combination of slow heating and fast cooling. Thus, tensile stresses of both scenarios act in series and are therefore additive to each other. The resulting total stress may become critical causing the formation of hairline cracks along peripheral grouts. Indeed, such hairline cracks can be observed in the field (Fig. 3 in [17]). However, the exact time of their initiation as micro-cracks cannot be estimated.

One approach to reduce critical stresses is to lower the elastic modulus of the mortars. Technically this goal can be achieved by increasing significantly the amount of redispersible powder by a factor of 2–3 to be in the range of 6–9 wt% redispersible powder. As a great advantage of numerical modeling, this effect can be simulated by reducing the elastic modulus of the adhesive and grouting mortars. Figure 10 shows the

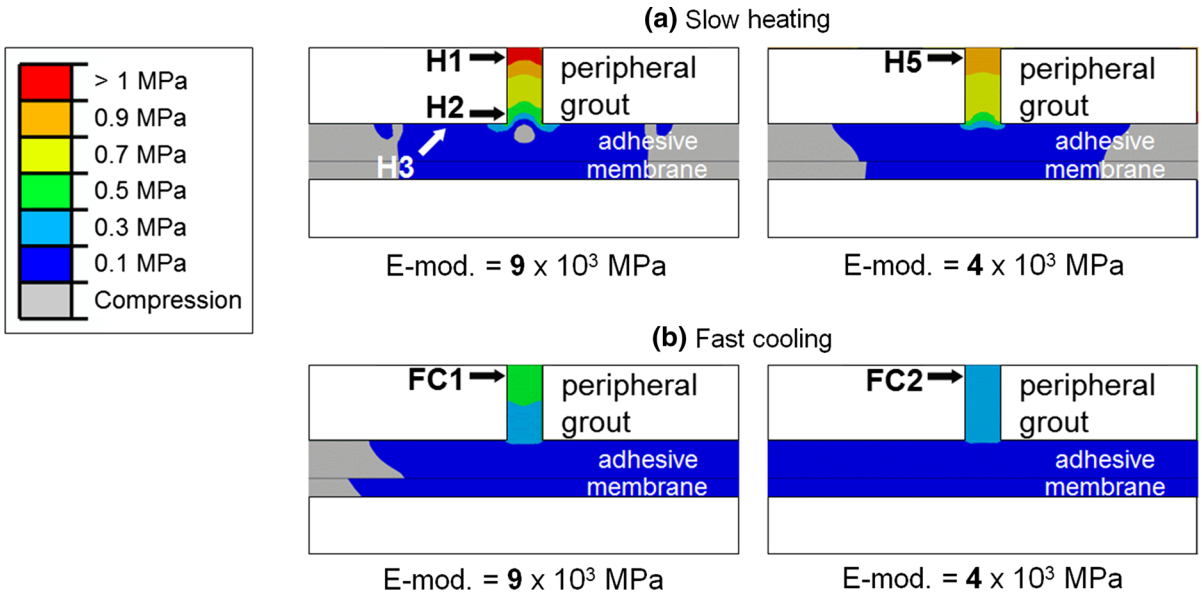

Fig. 10 Influence of the elastic modulus of the adhesive and grouting mortars onto thermally induced stresses in peripheral grouts during (**a**) slow heating by 30 °C and (**b**) fast cooling by 2 °C

stress distribution in peripheral grouts as a function of such a variation in the elastic modulus. Lowering the elastic modulus by a factor of two can reduce tensile stresses by *c*. 20 % (see curves H5 in Fig. 8a and FC2 in Fig. 11). A lower elastic modulus reduces stresses in both scenarios, slow heating and fast cooling, and will therefore reduce thermal stresses caused by a late afternoon rain storm.

The stress-temperature curves of Fig. 11 show that a fast cooling of the tile by 2 °C generates tensile stresses in peripheral grouts of about 0.4 MPa. In contrast, fast heating, as it may occur when a shadow (of a tree or a building, which cooled a tiling) passes by and the sun hits with its full power the tiling at a high inclination angle, does not generate high stress concentrations.

This result of the numerical modeling approach is of further interest with respect to the intensity of such extreme events. For example, on October 29th 2010, the authors observed a flash-heating event on a tiled wall exposed to SE. At that time in the year, the leaves were still at the trees, which kept the wall tiling in their shadow until 11:10 h. Then, of a sudden, the sun came out and hit the SE wall at a high inclination angle. The surface of the wall tiling warmed up by 14 °C within less than 12 min, providing a heating rate of 1.2 °C/min. However, flash cooling can be even more extreme. On May 11th 2010 a very strong hail-storm occurred,

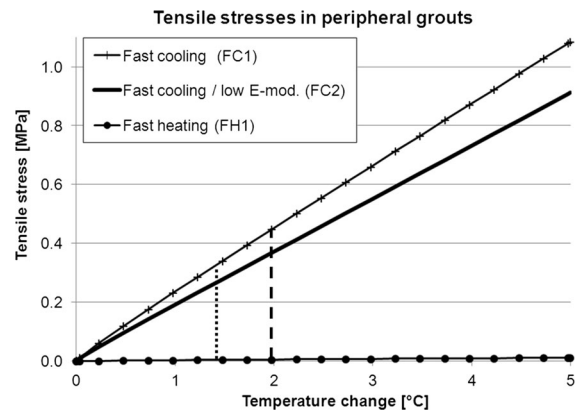

Fig. 11 Temperature-stress curves in peripheral grouts caused by fast cooling and fast heating. The locations FC1, FC2 and FH1 are indicated in Figs. 9 and 10. Dashed and stippled lines mark a 1.4 and 2 °C temperature change, respectively

which hit the different wall as well as floor tilings of the field experiment (see Fig. 11b and c in [17]). At 15:25 h the wall and floor tiles showed temperatures of 29 and 33 °C, respectively. Cold winds and accompanied rain cooled both wall and floor within 30 min down to 20 and 22 °C, respectively. Then, heavy hail started and accumulated on the floor tiling. The presence of iced-water caused an additional cooling of the floor by 18 °C within 20 min. All together, the floor temperature reduced from 33 °C

down to 5 °C within 50 min, while the wall cooled from 29 °C down to 14 °C, only. The maximum cooling rates reached in wall and floor were 0.46 and 1.86 °C/min, respectively.

Thus, fast cooling can be much more intense than fast heating because conductive heat transport by cold rain-water and hail ice is very efficient.

Figure 12 shows the relationship between the maximum rates of heating/cooling of tile surfaces versus the corresponding delta-*T* (temperature difference between inside of tile and mortar layer) of selected events (same field data as shown in Fig. 6). Heating events plot in the upper right quadrant, and cooling events plot in the lower left quadrant. At the origin of the coordinate system (0,0) there is no thermal stressing and the system is mechanically relaxed. The further away an event plots from the coordinate system's origin, the higher is the thermal load. The highest rates of normal daily heating and nightly cooling during the different seasons are between 0.2 and 0.3 °C/min and they produce delta-*T* values of maximum 1.4 °C. The data indicate that the correlation curve (stippled line in Fig. 12) is flattening towards higher rates of heating and probably also towards higher rates of cooling. Unfortunately, the delta-*T* values of the two extreme events (flash heating with 1.2 °C/min and hail storm with −1.86 °C/min) were not recorded, but it is assumed that they produce delta-*T* values in the order of 2–3 °C.

The field study was mainly carried out on tilings consisting of beige porcelain tiles. Hence, the thermal data is valid in a first manner for bright tilings. In addition, different tile materials were fixed on the SE wall and their expansion/shrinkage during thermal

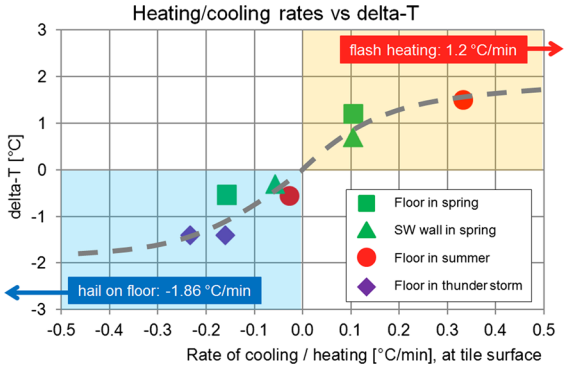

Fig. 12 Rate of temperature change (heating or cooling) at the tile surface versus the difference in temperature between tile and mortar for typical events selected from year 2009. For further explanations see text

loading was investigated. Table 2 summarises their thermal expansion coefficients as they were measured in the laboratory, and the maximum daily surface temperatures, which were reached on the 22nd of March 2011. Dark porcelain becomes 6 °C warmer than bright porcelain. During a hot summer day, the temperature difference between bright and dark porcelain might reach 10 °C.

For some field experiments, Wetzel et al. [17] took float glass as an analogue material for porcelain tiles. These glass plates allowed the direct observation of the adhesion interface to the mortar, its wetting structures and different stages of delamination. However, glass has very different thermal and adhesion properties, which amplify thermal loads and accelerate failure mechanisms [22]. Therefore, any comparison between porcelain and glass must be carried out in a differentiated way. This is also underlined by temperature measurements in the field. On the 22nd of March 2011 the glass plate reached the same temperature than the bright porcelain (Table 2). In contrast, on the 29th of October 2010, when the sun inclined at a higher angle, the glass plate heated up even more than the dark porcelain. Thus, in any situation the product of thermal coefficient (column 1 in Table 2) and material temperature (column 2 in Table 2) is a measure for the thermal expansion (column 3 in Table 2), which gives highest values for the glass, followed by the dark and the bright porcelain. Semi-vitrified ceramic tiles (here an intermediate color) and natural stones indicate lowest thermal expansion values and would suffer therefore the lowest thermal loads.

An important observation of this study is that the temperature gradients are extremely high towards the tile's surface and become quite small at the interface to the mortar. This explains why thermal stresses at the interface are relatively small and do not necessarily lead to failure under normal conditions, particularly not when tile installation was carried out according to common recommendations. The fact that thermal effects are reduced at the interface is also shown by thermal expansion data of Yiu et al. [18]. They measured a thermal expansion at the tile surface of 0.26 mm/m while the tile-adhesive interface shows an expansion of only 0.14 mm/m while the adhesive-concrete interface reveals an even smaller expansion of 0.07 mm/m. Thus, within the 7 mm thin tile the strain gradient is much larger (0.017 m^{-1}; mm/m per

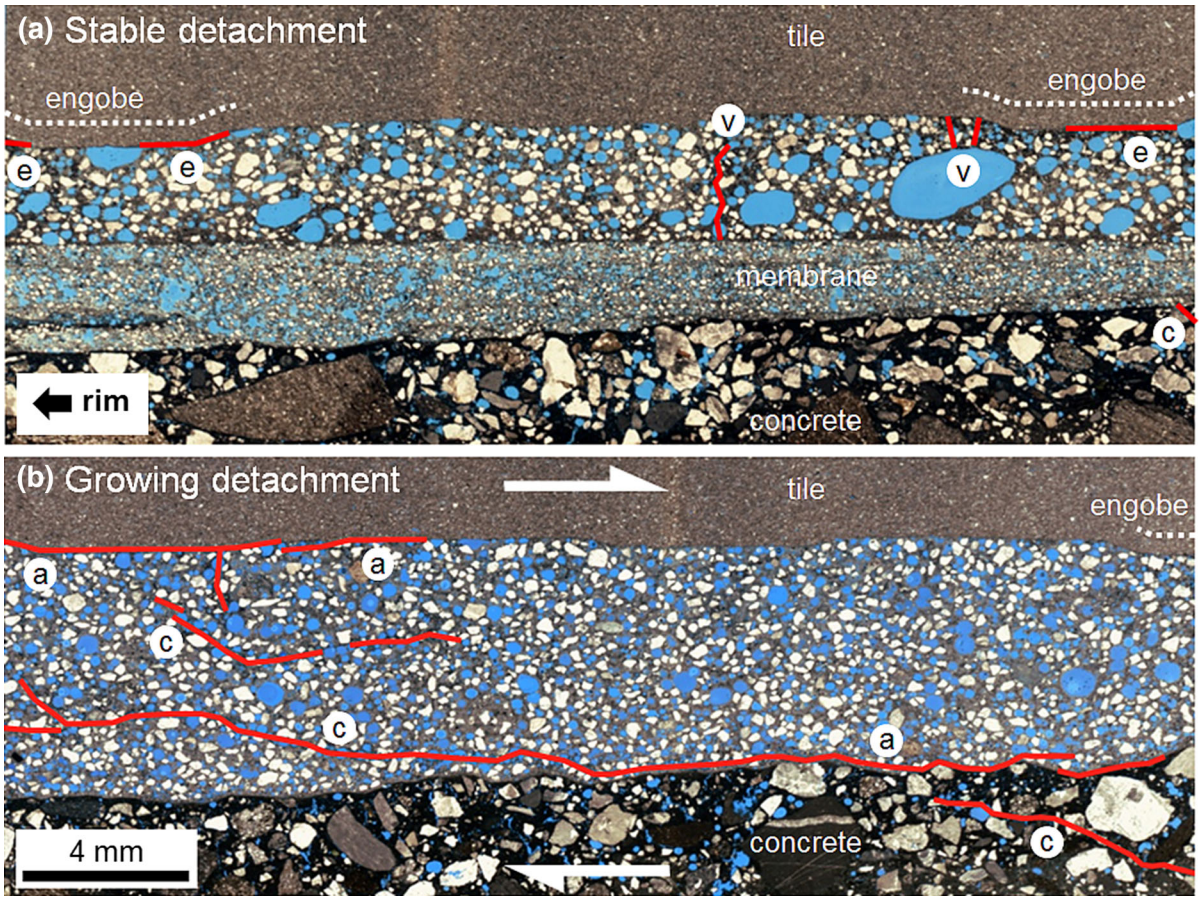

Fig. 13 Micrographs of sections tile-substrate from two types of detachments at the periphery of exterior balcony tilings (each measuring 167 cm × 273.2 cm; composed of porcelain tiles, 30 cm × 30 cm with 4 mm grout in between). **a** Stable detachment at the rim of the tiling field containing a flexible waterproofing membrane (sample taken from tile #10 located in Fig. 2b). **b** Growing detachment at the rim of the tiling field without a flexible waterproofing membrane (sample taken from tile #20 located in Figs. 1c and 2d). *a* adhesion crack, *e* adhesion crack along engobe, *c* oblique cohesion crack in mortar and concrete, *v* vertical cohesion crack in mortar. (For explanations see text.)

mm distance) compared to the strain gradient across the adhesive layer (0.0027 m^{-1}), which is probably due to corresponding temperature gradients as observed in our study.

An open question remains with respect to ultra-thin ceramic tiles showing thicknesses of 3 mm, only. Are the temperature gradients within thin tiles even larger and what are the resulting temperature gradients and resulting thermal stresses at the interface to the mortar?

Based on the annual time–temperature history (data of Fig. 6) one can estimate the frequency of the specific thermal events. For a bright porcelain floor tiling *c*. 450 thermal events with a delta-*T* of 0.5 °C occur per year. 250 events have delta-*T* values in the order of 1 °C, and only about 30 events reach delta-*T* values of 1.5 °C. For dark tiles heat absorption and resulting delta-*T* values will be higher.

Severe cracking in real outdoor systems can lead to adhesion failure. In this context, the numerical models indicate that application of a flexible waterproofing membrane can be crucial. In both situations, with (Fig. 13a) and without (Fig. 13b) a flexible waterproofing membrane, the tiles at the periphery of the tiling field can partly detach (compare Fig. 2b and d) because of the peripheral stress concentrations during cyclical heating and cooling (Fig. 7). Each cracking results in a local stress release. Hence it is crucial to prevent renewed stress increase promoting the

propagation of an existing crack. In this light, a flexible waterproofing membrane plays a key role. Its low elastic modulus (Table 1) allows deformation at the substrate-mortar interface, which, as a result, is less stressed. This stress reduction seems to be significant in terms of a low crack propagation rate. In other words, the early-formed local detachments along the periphery of the tiling field do not grow in size. The corresponding micrograph (Fig. 13a) reveals that even existing (i) adhesion and (ii) cohesion cracks do not propagate, thus, remain stable. Note that this "stable detachment" developed 21 months after the tiling was installed. From the beginning it was c. 45 cm^2 large and did not grow further until it was sampled 12 months later. (i) The adhesion cracks occur exactly at locations where the tile's rear side is coated by an engobe (marked by "e" in Fig. 13a). Our finding confirms observations of Pass and Zurbriggen [11]. These studies suggested that if porcelain tiles are embedded by the floating technique, such engobes are potential sites of adhesion cracking. (ii) The cohesion cracks are typically perpendicular to the mortar bed (marked by "v" in Fig. 13a) and are elsewhere described as early formed drying cracks (see Figs. 7c and 12a in [16]; Figs. 3e and 7b in [17]; Figs. 2 and 3 in [23]; Fig. 10 in [5]. Also these early drying cracks do not propagate further.

However, in cases where the flexible waterproofing membrane is lacking, small detached areas along the rim of tiling fields continue to grow until the stage for potential damage is reached. Here tiles can break and fall off. Half-cut tiles tend to be more sensitive for this type of failure (Fig. 2d). Note that the "growing detachment" shown in Fig. 13b developed 14 months after the tiling was installed. Initially it was relatively small but grew larger in the following 7 months (until it was sampled) to reach a size of *c*. 200 cm^2. In the context of propagating detachments, the microstructures of Fig. 13b can be interpreted as following: The microstructures reveal conjugated sets of interface parallel adhesion cracks (marked by "a" in Fig. 13b) and oblique cohesion cracks (marked by "c" in Fig. 13b). The latter intersect the mortar substrate boundary. The orientation of the oblique cohesion cracks (form upper left to lower right) indicates a dextral sense of shear caused by a relative expansion of the substrate with respect to the tiles. Such a scenario can either be related to a hygrical swelling of the substrate (caused by water ingress during a rain period), or a thermal shrinkage of the tiles (caused by rapid cooling during a rain/hail storm). Both, field measurements and numerical modeling indicate that a late afternoon summer hail storm represents the most extreme thermal loading. The fast thermal contraction of the cooling tiles on top of the warm substrate would deliver exactly the right scenario to propagate a conjugated crack system as it can be observed here.

5 Conclusions

The key parameters defining the effects of thermal loads in outdoor tilings can be subdivided into (i) material properties, (ii) application parameters and (ii) outdoor exposure factors.

(i) *Material properties* The types of mortar (adhesive and grouting mortars), especially their elastic moduli, significantly influence the build-up of thermal stresses. Flexible mortars (e.g., with an increased amount of redispersible powders) can reduce tensile and shear stresses at the adhesion interfaces to the tile. The latter is characterised by its material and color. Natural stones and semi-vitrified tile materials have smaller thermal expansion coefficients than porcelain ceramics. If porcelain is the material of choice, a dark color should be avoided for outdoor applications, because the dark color induces a "thermal expansion" [= (increase in temperature) × (thermal expansion coefficient)] almost twice as high compared to a bright semi-vitrified ceramic (Table 2). Previous investigations already showed that the size of the tile is critical with respect to stresses (e.g., [2]). The larger the tile size, the larger the total shrinkage to be accommodated during differences in relative expansion/contraction between mortar and tile and the higher the stress concentrations. In our study, we excluded variations in tile size and mainly focused on the size of the tiling field (see following paragraph).

(ii) *Application parameters* Numerical modeling clearly shows that the size of the tiling field has an enormous influence onto the thermal stresses. In our models the tiling field has a

width of 2.73 m and tensile/shear stresses increase from centre to rim (or in the opposite direction). Stress concentrations in the order of 1 MPa can be reached in the mortar. Keeping the field size of tilings small is therefore a very efficient way to reduce the magnitude of thermal stresses. Furthermore, the application of a flexible waterproofing membrane is important. Given by its low elastic modulus it can easily deform and relax the system, in particular the substrate-mortar interface. Especially in combination with daily thermal cycles the flexible waterproofing membrane can prevent fatigue failure and provide a durable outdoor performance.

The numerical models further indicate that a slow heating/cooling of the entire tiling system including its substrate by 15 °C causes tensile/shear stresses of about 0.5 MPa, which can already become critical on a long-term. From that point of view, outside temperatures during application and curing of the tile installation ideally should be around the annual mean temperature. Otherwise, hot summer temperatures or cold winter temperatures might induce thermal stresses above 0.5 MPa. Thus, for the mid European transitional climate the theoretically ideal application and curing temperature would be around 15 °C. Note that wind and direct sunlight exposure during tile installation should be avoided in any case, because both accelerate skin formation and reduce adhesion properties, the so-called Open Time performance [1].

(iii) *Exposure factors* The significantly larger day-night temperature differences during spring and summer compared to fall and winter (Figs. 3, 6) cause more intense cycles of thermal loading during the warm seasons. Consequently, the crack propagation rates of detached areas underneath tiles are largest in spring and summer [17]. Sheltering by roofs or full exposure of terrace and balcony tilings result in different stress-time loadings over the year. Uncovered floor tilings experience in summer the largest daily temperature differences, because both, the sun inclination angle and the intensity of sun radiation are highest. The delta-T values (difference in temperature between inside of tile and mortar) reach in the warm season 1.5 °C (morning heating) and late afternoon rain storms cause delta-T values of −1.5 °C. The numerical stress calculations suggest that a rain/hail storm on pre-heated floor tilings creates the largest thermal stresses, because the preheating and the fast cooling by the storm cause tensile stresses, which are additive. Under such circumstances, the total sum of tensile and/or shear stresses in peripheral grouts can reach up to 0.9 MPa, which is very critical with respect to the adhesion strength of grouting mortars. It is very likely that such an event may cause the formation of hairline cracks in the grouts, which might lead into further failure.

Wall tilings are very dependent on their exposure. South walls can experience their largest temperature changes in late fall, winter and early spring, when the nights are very cold and sun radiation can be very intensive because the sun inclines with a high angle onto it.

Large shadows of trees, neighboring building, topographic elevations or clouds can cause rapid cooling and heating but have little effect onto the delta-T value (difference in temperature between inside of tile and mortar) because of the thermal inertia of the system.

Having made the observations that the thermal gradients are highest towards the tile's surface an open question remains with respect to ultra-thin ceramic tiles, showing thicknesses of 3 mm only. Are the temperature gradients within thin tiles even larger and what are the resulting temperature gradients and resulting thermal stresses at the interface to the mortar?

Acknowledgments We thank Andrea Greminger, Alexander Wetzel (Univ. of Bern) and Monika Stocker (Akzo Nobel Chemicals AG) for support in the acquisition of field data, Josef Kaufmann (Empa) for advice in temperature data logging and Ralph Mettier (Univ. of Bern) for the introduction in numerical modeling with ABAQUS. Financial support by Swiss Commission for Technology and Innovation is gratefully acknowledged (CTI project No 8605.1 EPRP-IW).

References

1. Bühler T, Zurbriggen R, Pieles U, Huwiler L, Raso R (2012) Dynamics of early skin formation of tiling mortars

investigated by microscopy and diffuse reflectance infrared Fourier transformed spectroscopy. Cement and Concrete Composites 37:161–170
2. Felixberger JK (2005) Spannungen im Verbundsystem: Fliese—Verlegemörtel—Untergrund. In: Verein Deutscher Ingenieure VDI (ed) Jahrbuch 2005 Bautechnik. VDI—Verlag GmbH, Düsseldorf, pp 359–390
3. Gao J, Chung DDL (2002) Damage evolution during freeze–thaw cycling of cement mortar, studied by electrical resistivity measurement. Cem Concr Res 32:1657–1661
4. Hazaree C, Ceylan H, Wang K (2011) Influences of mixture composition on properties and freeze–thaw resistance of RCC. Constr Build Mater 25:313–319
5. Herwegh M, Zurbriggen R, Mettier R, Winnefeld F, Kaufmann J, Wetzel A (2015) Hygrical shrinkage stresses in tiling systems: numerical modeling combined with field studies. Cem Concr Compos 35:1–10
6. Mahaboonpachai T, Kuromiya Y, Matsumoto T (2008) Experimental investigation of adhesion failure of the interface between concrete and polymer-cement mortar in an external wall tile structure under a thermal load. Constr Build Mater 22:2001–2006
7. Mahaboonpachai T, Matsumoto T, Inaba Y (2010) Investigation of interfacial fracture toughness between concrete and adhesive mortar in an external wall tile structure. Int J Adhes Adhes 30:1–9
8. Metha PK, Burrows RW (2001) Building durable structures in the 21st century. Concr Int 23:57–63
9. MeteoSchweiz (2014) http://www.meteoschweiz.admin.ch/web/de/klima/klima_heute.html
10. Ndon U, Bergeson K (1995) Thermal expansion of concretes: case study in Iowa. J Mater Civ Eng 7:246–251
11. Passa DS, Sotiropoulou AB, Pandermarakis ZG, Mitsopoulos GD (2012) Thermal and drying cyclic loading for cement based mortars and expanded polystyrene foam layers. Appl Mech Mater 204–208:3648–3651
12. Sicat E, Gong F, Zhang D, Ueda T (2013) Change of the coefficient of thermal expansion of mortar due to damage by freeze thaw cycles. Journal of Advanced Concrete Technology 11:333–346
13. Toakley AR, Waters EH (1973) Stresses in ceramic tiling due to expansion and shrinkage effects. Building Sciences 8:269–281
14. Tonoli GHD, Santos SF, Savastano H, Delvasto S, Mejía de Gutiérrez R, del Lopez de Murphy M (2011) Effects of natural weathering on microstructure and mineral composition of cementitious roofing tiles reinforced with fique fibre. Cement Concr Compos 33:225–232
15. Weder C (1979) Neuentwickeltes mechanisch-induktives Setzdehungsmessgerät an der EMPA Dübendorf. Material und Technik 2:98–101
16. Wetzel A, Herwegh M, Zurbriggen R, Winnefeld F (2012) Influence of shrinkage and water transport mechanisms on microstructure and crack formation of tile adhesive mortars. Cem Concr Res 42:39–50
17. Wetzel A, Zurbriggen R, Herwegh M, Greminger A, Kaufmann J (2012) Long-term study on failure mechanisms of exterior applied tilings. Constr Build Mater 37:335–348
18. Yiu CY, Ho DCW, Lo SM (2007) Weathering effects on external wall tiling systems. Constr Build Mater 21:594–600
19. Zentralverband Deutsches Baugewerbe (2005a) Aussenbeläge—Belagskonstruktionen mit Fliesen und Platten ausserhalb von Gebäuden. Merkblatt ZDB
20. Zentralverband Deutsches Baugewerbe (2005b) Verbundabdichtungen. Merkblatt ZDB
21. Zurbriggen R, Wetzel A, Greminger A, Kaufmann J, Pass K, Waser H (2009) Outdoor tile damages: a study on critical parameters and characteristic microstructures. Proceedings of the IDMMC two, 30th March 2009, Nuremberg, Germany, pp 18–24
22. Zurbriggen R, Pass K, Wetzel A (2011) Gut verlegt hält länger. Fliesen und Platten 2:18–21
23. Zurbriggen R, Herwegh M, Wetzel A (2012) Hygrical stresses in tilings: a combined field, microstructural and numerical modeling study. In: Proceedings of the conference of the chemistry of Construction Materials Division (Fachgruppe Bauchemie, GDCh), Dübendorf, Switzerland, 11–12 Oct 2012, Monographie, 45, pp 103–108